

Supporting Information

In situ Nitroso Formation Induced Structural Diversity of Uranyl Coordination Polymers

Xiang-He Kong,^{†[a,b](#)} Kong-Qiu Hu,^{†[b](#)} Qun-Yan Wu,^b Lei Mei,^b [‡] Ji-Pan Yu,^b Zhi-Fang Chai,^{b,c} Chang-Ming Nie*,^a and Wei-Qun Shi*^b

[a] School of Resource and Environment and Safety Engineering, University of South China, Hengyang, Hunan, 421001, China

[b] Laboratory of Nuclear Energy Chemistry, Institute of High Energy Physics, Chinese Academy of Sciences, Beijing 100049, China

[c] Engineering Laboratory of Advanced Energy Materials, Ningbo Institute of Industrial Technology, Chinese Academy of Sciences, Ningbo, Zhejiang, 315201, China.

[†] The first two authors contributed equally to this work.

S1. Figures

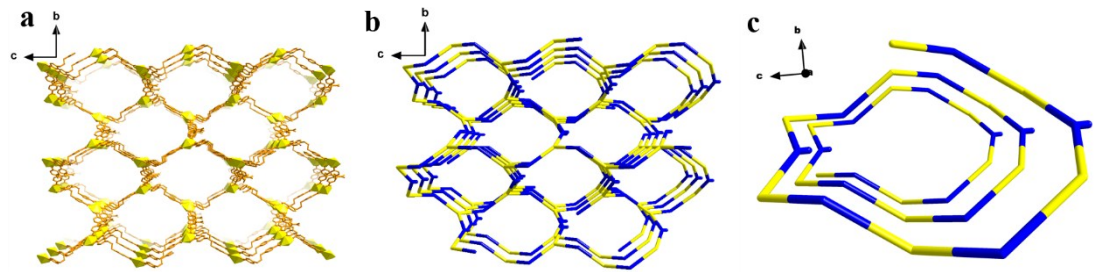


Fig. S1 (a) The 3D framework along the *a*-axis of compound 1. (b) The simplified 3D topology networks. (c) The spiral structure of compound 1.

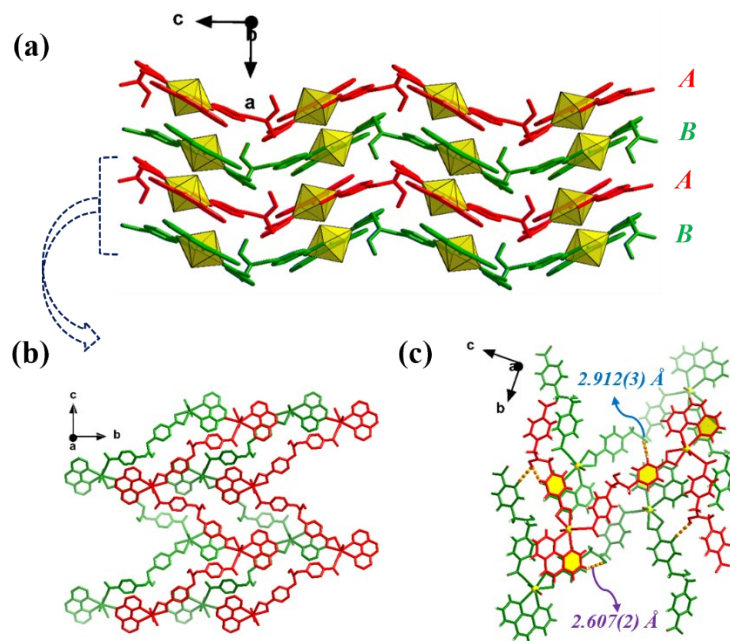


Fig. S2 (a) The neighboring 2D wavy layers adopt *ABAB* stacking mode to extend to 3D structure of compound 3. (b, c) The hydrogen bonding and π - π interaction between the adjacent layers.

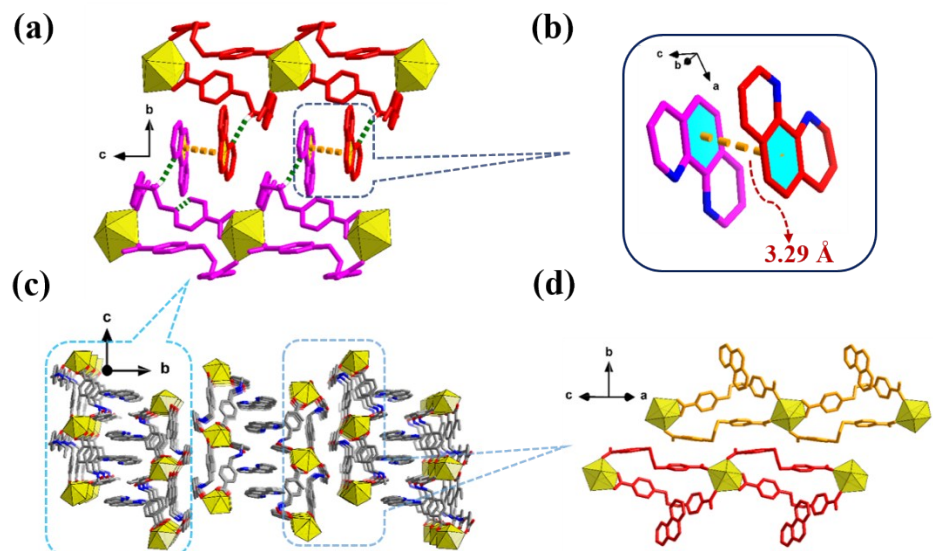


Fig. S3 (a) The interactions between the two groups of meso-compounds of compound 4. (b) The hydrogen-bonding interactions between the templating phen. (c) The stacking space of 3D structures. (d) The stacking mode between chain and chain of two adjacent layers.

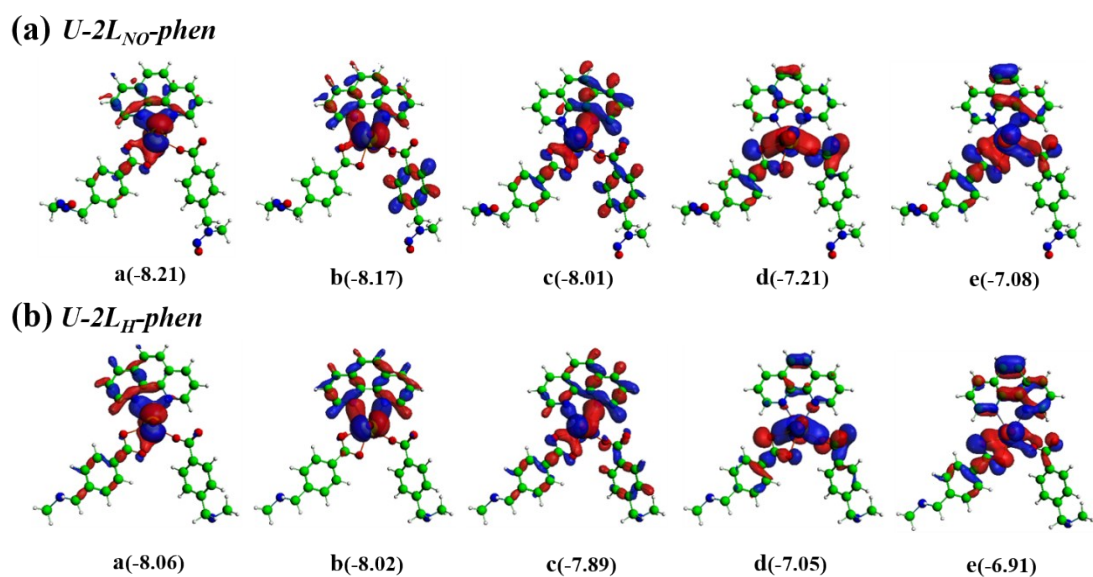


Fig. S4 Diagrams of canonical occupied MOs (a-e) and the corresponding MO energy (eV) for the complexes 3(a) and 3(b).

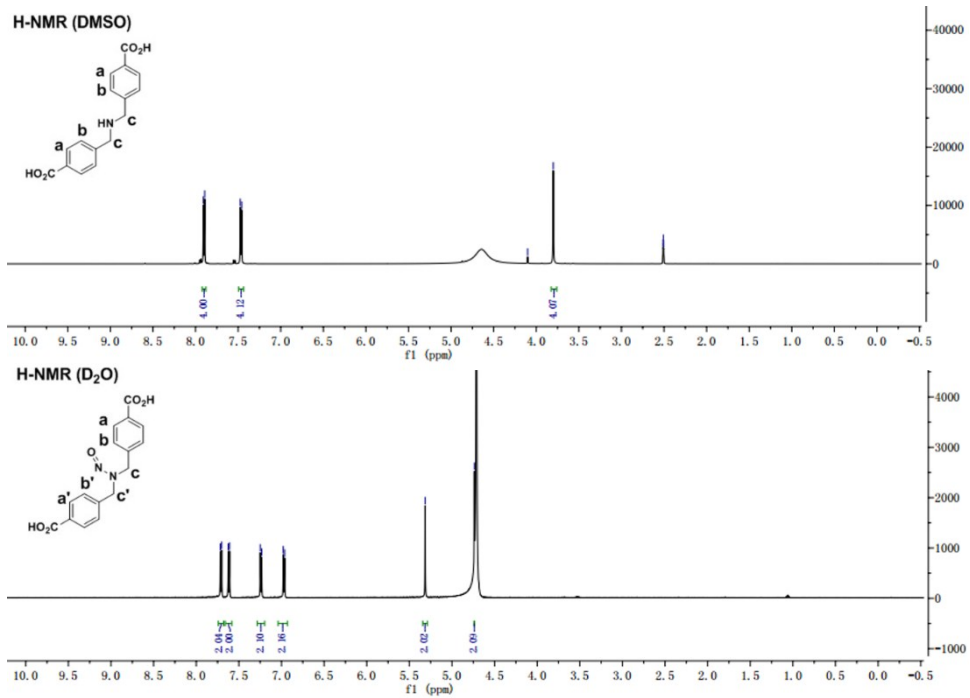


Fig. S5 ^1H NMR of H_2bcHba (top) in DMSO and H_2bcNOba (bottom) spectra in D_2O .

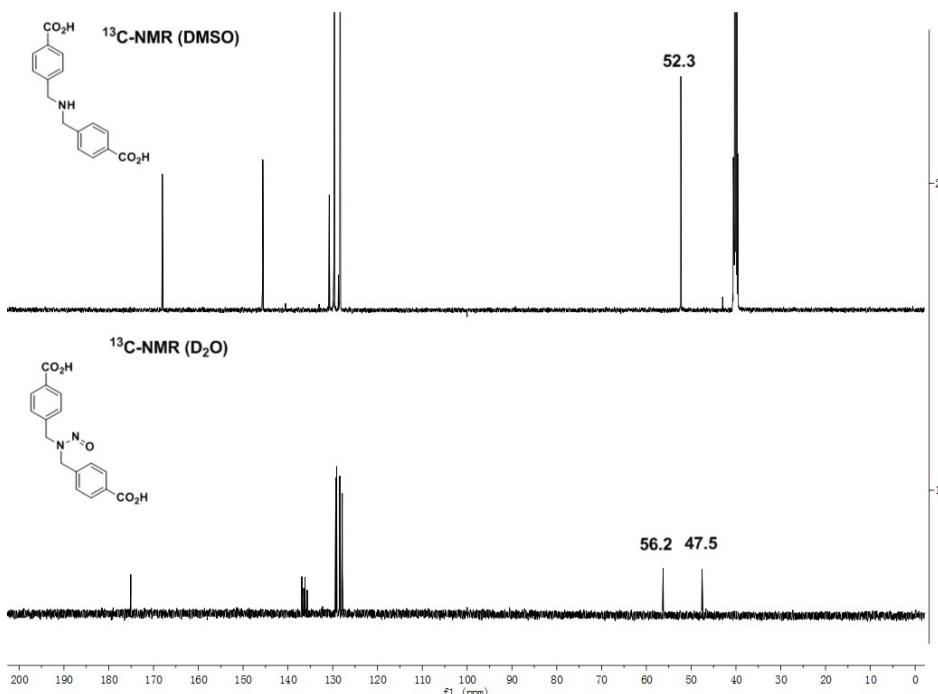


Fig. S6 ^{13}C NMR of H_2bcHba (top) in DMSO and H_2bcNOba (bottom) spectra in D_2O .

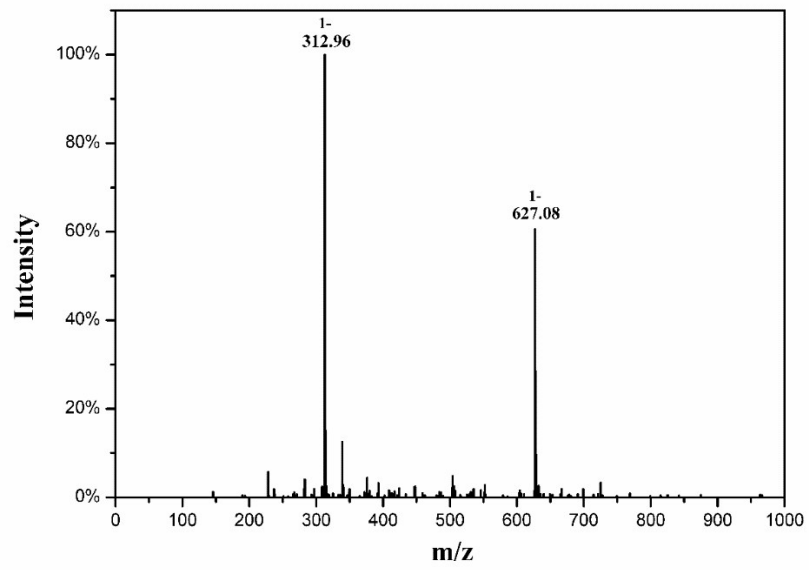


Fig. S7 ESI-MS spectrum of the ligand H_2bcNOba .

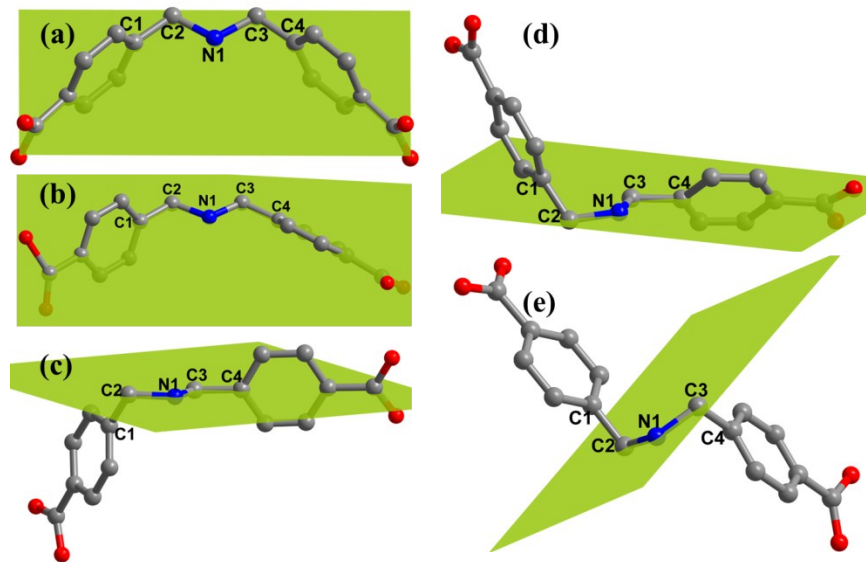


Fig. S8 The different configurations of ligand bcH_2ba^- in different structures: (a) L_b ; (b) L_a ; (c) in compound 1; (d, e) in compound 4.

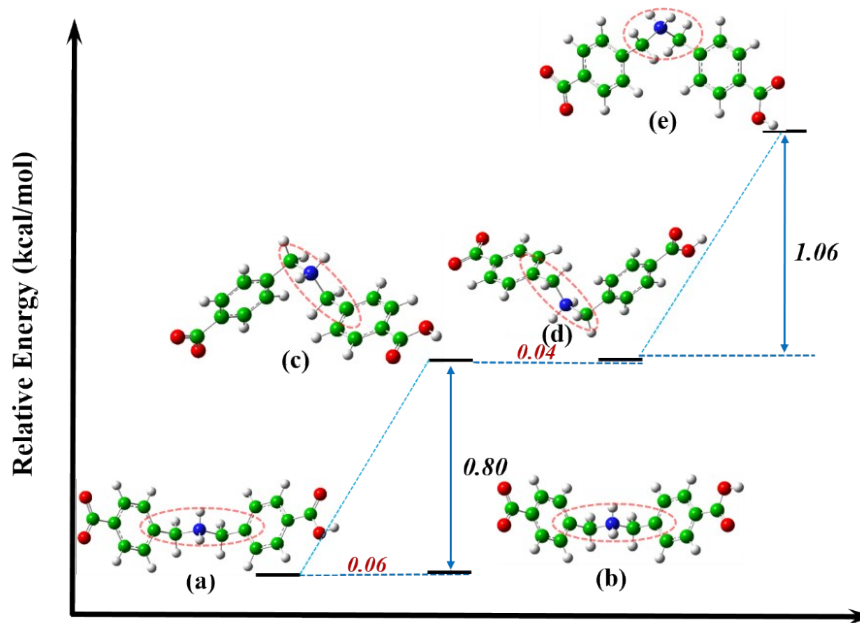


Fig. S9 The relative energy after optimization of five configurations of ligand HbcH₂ba.

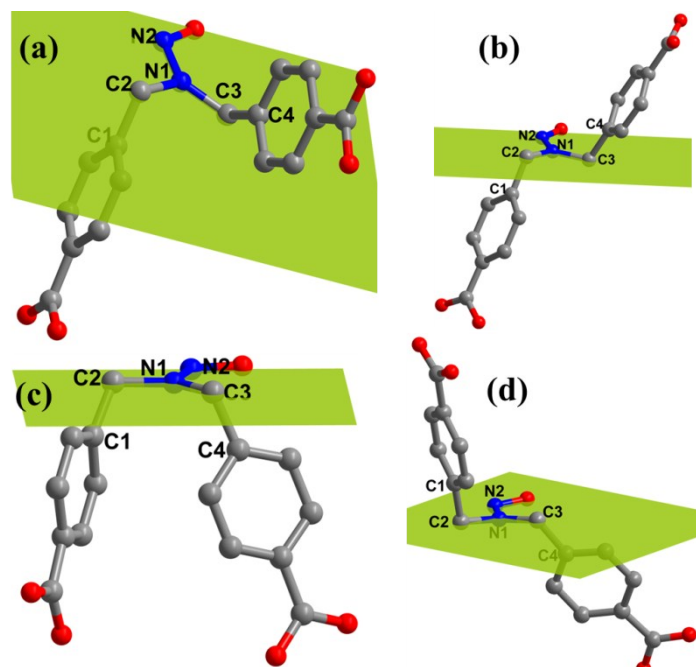


Fig. S10 The different configurations of ligand bcNOBa²⁻ in different structures: (a) L_c; (b) in compound 1; (c) in compound 2; (d) in compound 3.

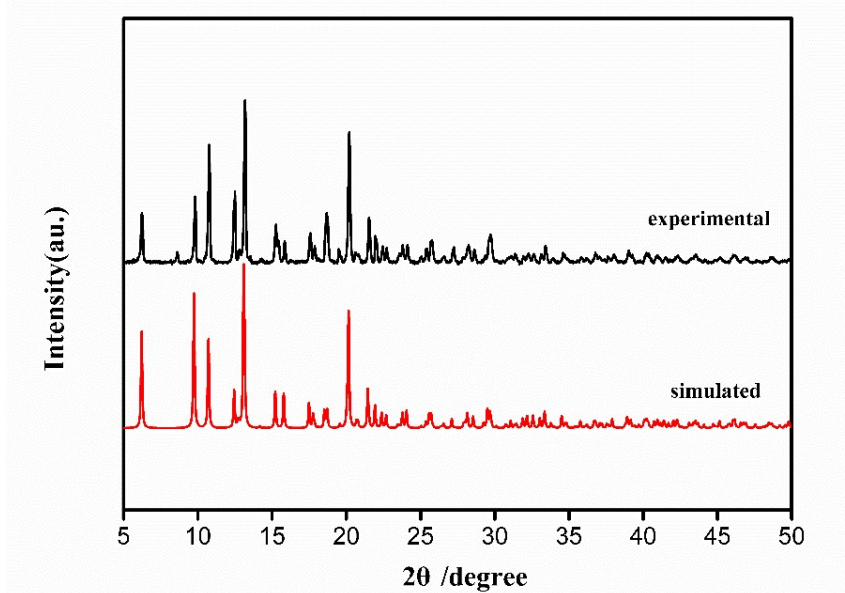


Fig. S11 The PXRD patterns of the compound 1

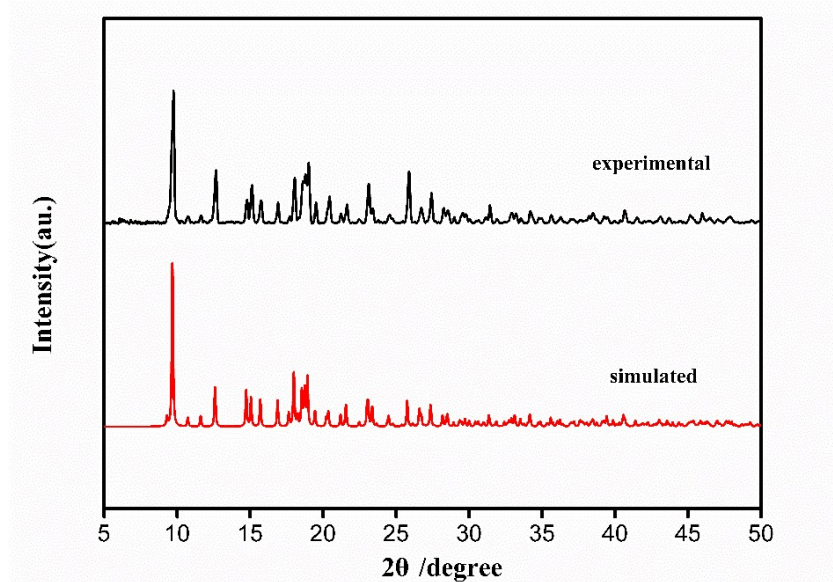


Fig. S12 The PXRD patterns of the compound 2

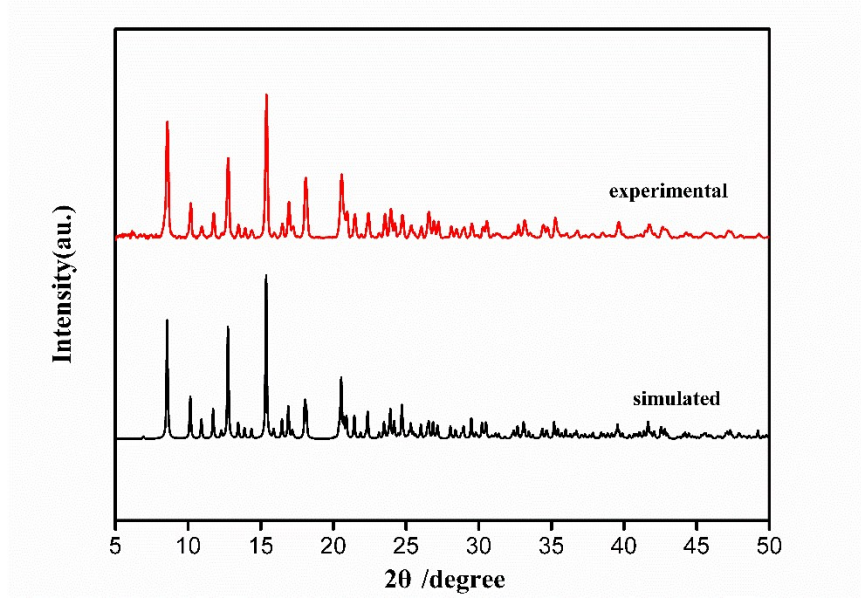


Fig. S13 The PXRD patterns of the compound 3

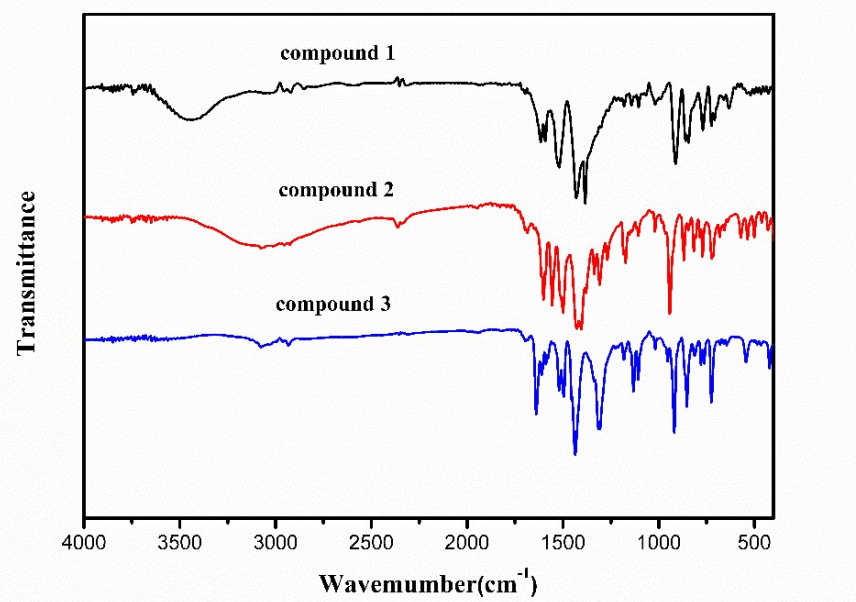


Fig. S14 The IR spectra of compounds 1-3.

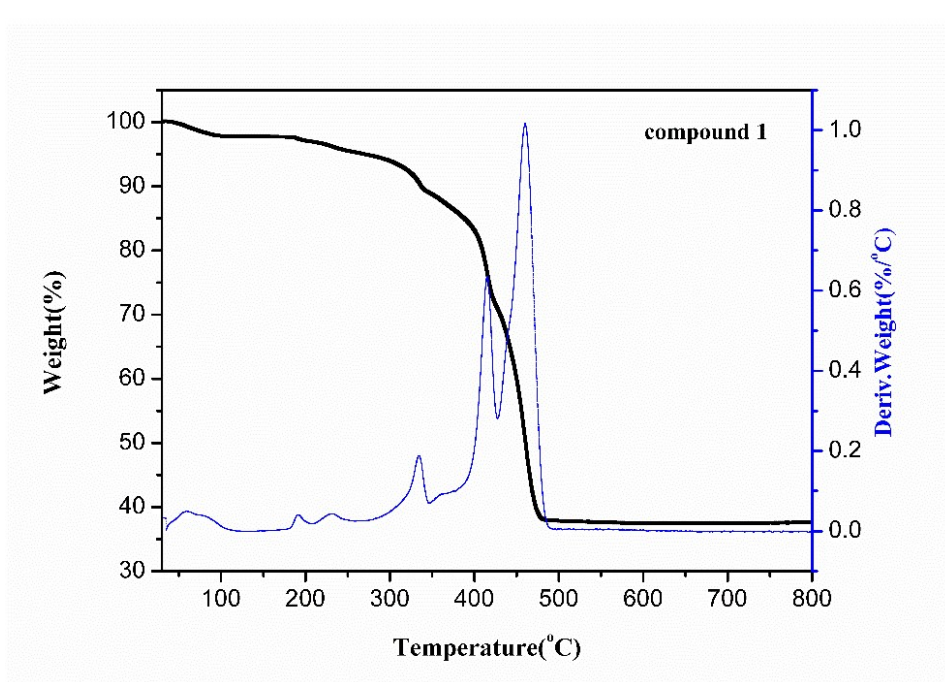


Fig. S15 The TGA diagrams of compound 1.

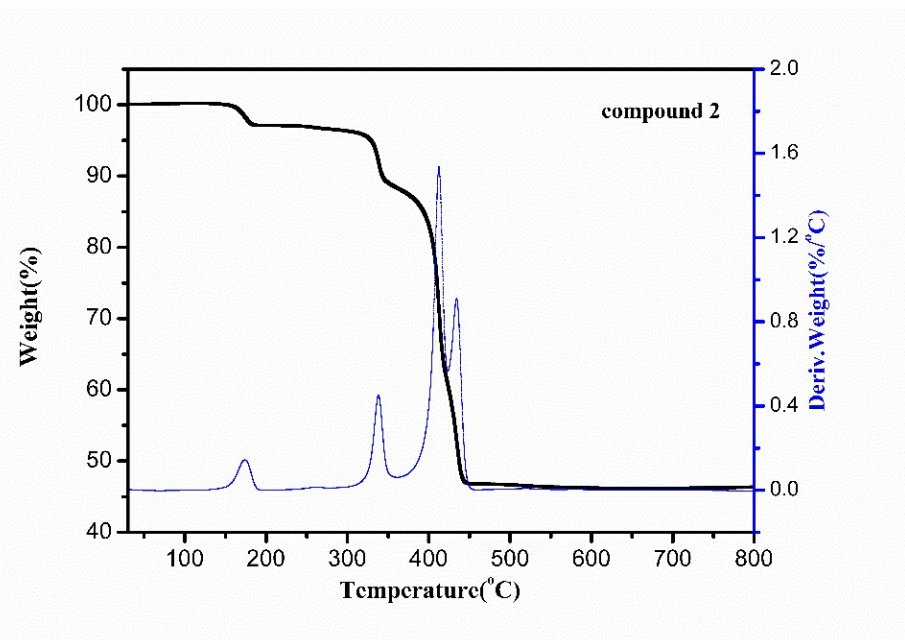


Fig. S16. The TGA diagrams of compound 2.

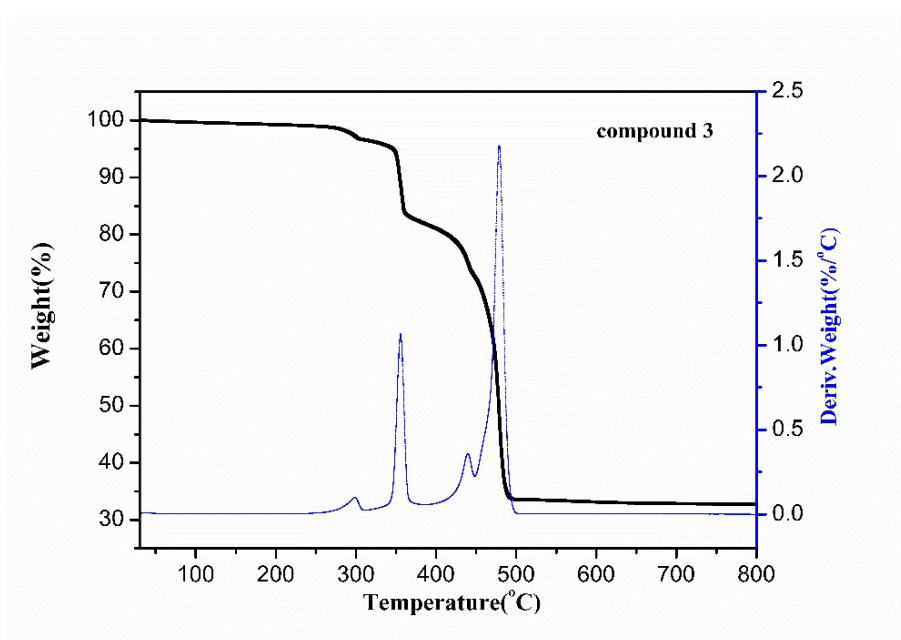


Fig. S17. The TGA diagrams of compound 3.

S2. Tables

Table S1 Selected Calculated and Crystal Bond Distances (\AA) of the U-O Bonds, Wiberg Bond Order (WBIs), and the Electron Density (ρ , au) its Laplacian ($\nabla^2\rho$) at U-O Bond Critical Points (BCPs) for Compound 1.

Compound 1		U1=O1	U1=O2	U1-O3	U1-O4	U1-O5	U1-O6	U1-O7	U1-O8	O1-U1-O2
Bond	Calc.	1.793	1.793	2.477	2.481	2.486	2.484	2.482	2.488	179.916
Distances	Exp.	1.745(9)	1.772(10)	2.512(8)	2.431(9)	2.438(8)	2.476(8)	2.460(8)	2.517(8)	178.5(4)
WBIs		2.165	2.168	0.496	0.494	0.425	0.426	0.451	0.446	
ρ		0.2856	0.2857	0.0572	0.0566	0.0557	0.0564	0.0559	0.0561	
$\nabla^2\rho$		0.3055	0.3055	0.188	0.186	0.1831	0.1856	0.1838	0.1846	

Table S2 Selected Calculated and Experimental Bond Distances (\AA) of the U-O Bonds, Wiberg Bond Order (WBIs), and the Electron Density (ρ , au) its Laplacian ($\nabla^2\rho$) at U-O Bond Critical Points (BCPs) for Compound 2.

Compound 2		U1=O1	U1=O2	U1-O3	U1-O4	U1-O5	U1-O6	U1-O7	O1-U1-O2
Bond	Calc.	1.786	1.786	2.432	2.456	2.349	2.328	2.515	178.654
Distances	Exp.	1.757(5)	1.753(4)	2.437(4)	2.486(4)	2.294(4)	2.312(4)	2.402(4)	177.7(2)
WBIs		2.185	2.19	0.501	0.474	0.613	0.593	0.370	
ρ		0.2991	0.2991	0.0619	0.0553	0.0716	0.0674	0.0418	
$\nabla^2\rho$		0.2893	0.2893	0.207	0.1844	0.3365	0.2929	0.1483	

Table S3 Selected Calculated and Experimental Bond Distances (\AA) of the U-O Bonds, Wiberg Bond Order (WBIs), and the Electron Density (ρ , au) its Laplacian ($\nabla^2\rho$) at U-O Bond Critical Points (BCPs) for Compound 3

Compound 3		U1=O1	U1=O2	U1-O3	U1-O5	U1-O6	U1-N1	U1-N2	O1-U1-O2	N1-U1-N2
Bond	Calc.	1.789	1.789	2.249	2.452	2.435	2.625	2.600	177.384	63.62
Distances	Exp.	1.759(7)	1.775(7)	2.216(7)	2.456(6)	2.404(6)	2.569(7)	2.540(7)	176.4(3)	64.8(2)
WBIs		2.186	2.173	0.801	0.473	0.500	0.356	0.374		
ρ		0.2886	0.2892	0.0851	0.0607	0.0628	0.4739	0.0498		
$\nabla^2\rho$		0.3046	0.3048	0.3593	0.2025	0.2096	0.13	0.1373		

Table S4 Selected Crystal Bond Distances (\AA) of the U-O Bonds, Wiberg Bond Order (WBIs), and the Electron Density (ρ , au) its Laplacian ($\nabla^2\rho$) at U-O Bond Critical Points (BCPs) for Compound 4.

Compound 4		U1=O1	U1=O2	U1-O4	U1-O5	U1-O8	U1-O9	U1-O10	O1-U1-O2	
Bond	Distances	Exp.	1.788(3)	1.788(3)	2.306(3)	2.338(3)	2.332(3)	2.402(3)	2.572(3)	177.8(13)
WBIs			2.148	2.164	0.634	0.621	0.594	0.492	0.411	
ρ			0.285	0.2867	0.0771	0.0679	0.0717	0.0675	0.046	
$\nabla^2\rho$			0.3111	0.3046	0.3025	0.2968	0.2878	0.2289	0.1535	

Table S5 Percent Contribution of the Molecular Orbitals in Compound 1.

MOs	Element	Contributions of Each		
		O(2p)	U(5f)	U(6d)
a	U1			3.43
	O1	7.69		
	O2	20.89		
	O5	4.07		
	O6	4.49		
	O7	5.26		
	O8	5.75		
	O4	1.53		
b	U1			7.91
	O1	23.1		
	O2	20.47		
	O6	1.25		
	O7	2.37		
c	U1			1.6
	O1	13.23		
	O2	9.1		
	O6	1.76		
	O7	5.69		
d	U1		24.22	
	O1	22.79		
	O2	5.62		
	O5	1.67		
	O6	1.49		
	O7	3.32		
	O8	3.45		
e	U1		24.00	
	O1	30.67		
	O2	18.71		
	O7	1.22		
	U1			1.12
f	O1	9.56		
	O5	1.56		
	O6	4.57		
	O8	2.09		